Stanford Exploration Project, Report 115, May 22, 2004, pages 383–391

Shot-profile migration of GPR data

Jeff Shragge, James Irving, and Brad Artman[1]

ABSTRACT

Multi-offset ground-penetrating radar data possess a number of important advantages over constant-offset data, and are becoming increasingly popular within the GPR community. With the availability of these data comes the opportunity to experiment with state-of-the-art seismic imaging techniques. Here, we consider the application of shot-profile migration, a prestack scalar wave-equation imaging method, to 2-D multi-offset GPR data. With this method, source and receiver wavefields of individual shot records are propagated separately and combined at depth with application of an imaging condition. Receiver wavefields are comprised of recorded traces, and source wavefields are modeled from point sources at the transmitter locations. The complete migrated image is the sum of all overlapping shot-record migrations.

INTRODUCTION

At present, the majority of ground penetrating radar (GPR) work involves the collection, processing, and interpretation of constant-offset data. However, the increased availability of multi-channel GPR systems is making multi-offset data collection increasingly popular. Advantages of working with multi-offset GPR data include the improved estimation of subsurface velocities and imaging of reflectors, and also the ability to perform amplitude versus offset (AVO) or angle (AVA) analysis (Fisher et al., 1992a; Greaves et al., 1996; Baker, 1998). These advantages allow for better estimation of sedimentary facies and subsurface properties.

Because of the many similarities between the GPR and seismic methods, numerous exploration seismic imaging techniques have been directly transferred to the radar community. One family of imaging methods commonly used in seismic exploration, especially in areas of complex geology, is based on wave-equation wavefield extrapolation. Methods in this family employ a one-way scalar wave equation to extrapolate a wavefield recorded at the surface through a subsurface velocity model. In theory, this procedure generates the wavefield that would have been recorded had the instruments been located at a surface deeper within the earth. Images of geologic structure are then constructed through the evaluation of a physical imaging condition at each subsurface model point.

Here, we consider the application of shot-profile migration, a prestack imaging algorithm belonging to the family of scalar wave-equation methods, to 2-D multi-offset GPR data. This

[1]**email:** jeff@sep.stanford.edu, jdirving@pangea.stanford.edu, brad@sep.stanford.edu

method is similar to the zero-offset, survey-sinking migration method proposed by Sena et al. (2003), which involves using split-step Fourier operators to extrapolate GPR wavefields. However, the algorithm presented here is designed for application to multi-offset data in a shot-profile configuration, and allows for the easy formation of angle-dependent images that are suitable for migration velocity analysis (MVA) and AVA studies.

THEORY

Scalar Wave Equation for GPR Imaging

Modeling a GPR experiment is a complicated process that, for complete accuracy, requires taking into account such effects as antenna radiation patterns and the vectorial nature of electromagnetic (EM) wave propagation and scattering (van der Kruk et al., 2003). It is well known, however, that seismic processing techniques based on a scalar wave equation can often be applied very successfully to GPR data (Fisher et al., 1992b). This latter point is not mere coincidence. In many situations, isotropic scattering and scalar wave propagation effectively model the kinematics of a GPR experiment. Here, in applying an imaging algorithm based on a scalar wave equation to GPR data, we argue that radar propagation kinematics are well represented. In addition, we suggest that with further development, effects such as antenna radiation patterns and realistic scattering could be accounted for in the source and receiver wavefields and imaging condition.

Considering a situation where Maxwell's equations can be represented by a 2-D scalar wave equation involves making two approximations. First, we implicitly assume that the subsurface geology and sources are strictly 2-D. This results in the decoupled transverse electric (TE) and transverse magnetic (TM) propagation modes (Jackson, 1975). Choosing the TE-mode, we next assume that heterogeneities within the earth are small such that the gradients of EM constitutive parameters can be neglected (Sena et al., 2003). The result is a scalar wave equation for transverse electric field, E, which in the frequency (ω) domain is given by,

$$\left[\frac{\partial^2}{\partial z^2}+\frac{\partial^2}{\partial x^2}\right]E+\omega^2 s^2 E=0, \tag{1}$$

where the slowness of wave propagation (i.e. inverse of velocity), s, is dependent on the medium's dielectric permittivity, ϵ, and conductivity, σ, through,

$$s=\sqrt{\mu(\epsilon-\frac{i\sigma}{\omega})}\approx\sqrt{\mu\epsilon}. \tag{2}$$

The magnetic permeability of the medium, μ, is roughly constant for most material likely to be encountered in a routine radar application. Hence, in low conductivity media (i.e. $\sigma \ll \omega$), the slowness of wavefield propagation is directly proportional to the dielectric permittivity.

Shot-profile wavefield continuation

Assuming applicability of the scalar wave equation given by equation (1), the first step in GPR shot-profile migration is the extrapolation of surface-recorded data to depth. This is done by applying a one-way wave-equation operator to an arbitrary wavefield, as a function of space and frequency, to yield the wavefield at a deeper level:

$$W(z+\Delta z,x,\omega) = W(z,x,\omega)\, \mathrm{e}^{\pm k_z \Delta z}. \tag{3}$$

Here, the positive or negative exponent corresponds to causal or acausal propagation, respectively, and Δz is the size of the downward continuation step. The vertical wavenumber, k_z, is calculated from the scalar wave-equation dispersion relation,

$$k_z = \sqrt{s^2\omega^2 - k_x^2}, \tag{4}$$

where k_x is the horizontal Fourier wavenumber component of the data wavefield.

Surface-recorded wavefields are extrapolated to all depths within the model through successive applications of equation (3) using a vertical wave-number given by equation (4). Although equation (4) is strictly valid only for vertically stratified media, techniques exist to extend it to laterally varying media. We employ a split-step Fourier approach (Stoffa et al., 1990) that involves approximating k_z in equation (4) using a Taylor series expansion about a reference slowness, s_0:

$$k_z \approx \omega(s-s_0) + \sqrt{s_0^2\omega^2 - k_x^2}. \tag{5}$$

The first, mixed-domain term in equation (5) acts as a local correction to the second term that handles the bulk of the propagation. Increased accuracy can be achieved by summing the results of multiple reference velocity steps in order to minimize the quantity $s(x)-s_0$.

Shot-profile migration directly mimics the data collection process by migrating individual shot records. Receiver wavefields are comprised of individual shot profiles and are propagated acausally. Source wavefields have the same geometry, but are initially zero except for an appropriate source function at the transmitter location, and are propagated causally.

The imaging condition

The second step of shot-profile migration is forming a subsurface image through extraction of appropriate information from the independently extrapolated source and receiver wavefields. Claerbout's imaging principle (Claerbout, 1971) asserts that energy in the receiver wavefield, R, that is spatially collocated with energy in the source wavefield, S, at time $t=0$ originates from a reflector at that model point. Mathematically, this is accomplished through the extraction of the zero-lag of the cross-correlation of the two wavefields. In practice, this translates to a summation over frequency after the multiplication of the wavefields (Claerbout, 1985),

$$I(z,x) = \sum_s I_s(z,x) = \sum_s \sum_\omega S_s(z,x,\omega) R_s^*(z,x,\omega), \tag{6}$$

Here, $I(z,x)$ represents the image point as a function of horizontal distance and depth, * represents complex conjugation, and the subscript s refers to individual shot-profile image results.

Additional subsurface reflectivity constraints are obtained by extending (6) to include subsurface offset (Rickett and Sava, 2002). Offset domain common image gathers (ODCIGs) are created by multiplication of the source and receiver wavefields after a lateral shift of h:

$$I(z,x,h) = \sum_s I_s(z,x,h) = \sum_s \sum_\omega S_s(z,x+h,\omega) R_s^*(z,x-h,\omega). \tag{7}$$

Angle domain common image gathers

ODCIGs can be transformed into an angle domain representation (ADCIGs) that describe reflectivity as a function of incidence angle at the reflector, γ (Sava and Fomel, 2003). ADCIGs are generated after migration with the relation,

$$\tan\gamma = -\frac{k_h}{k_z}. \tag{8}$$

which uses the Fourier transformed wavenumbers associated with offset and depth.

Angle gathers may be used to examine the accuracy of the imaging velocity model at all subsurface locations. A reflector focused with the correct velocity model should be at a consistent depth for all illumination angles. Deviations in reflector position due to incorrect velocity models result in angle-dependent "smiles" and "frowns", which indicate over- and under-migration, respectively. Corresponding velocity model errors can be estimated from angular moveout through the process of migration velocity analysis (MVA). More importantly, after migration velocity inaccuracy has been minimized, angle-dependent amplitude variations should be attributed to AVA response. However, for GPR images, this will not be the case unless the proper radiation patterns and scattering physics have been taken into account.

APPLICATION TO FIELD DATA

We applied the shot-profile migration methodology outlined above to a 2-D multi-offset GPR data set collected near Langley, British Columbia, Canada. The geology of the field site consists of a sand and gravel glacial outwash deposit underlain by a conductive marine clay, the depth of which varies from near surface to approximately 10 m across the profile. The data were collected along a road using a PulseEkko 100 GPR system with 100 MHz antennas oriented perpendicular to the survey line. A shot-profile survey configuration was used with 30 receiver offsets ranging from 0.5 m to 15 m, with a step size of 0.5 m. The transmitter spacing along the line was also 0.5 m, with a total of 200 shot gathers making up the approximately 100 m long profile.

Pre-processing of the Langley data included residual median filtering to remove the low frequency inductive response upon which the radar reflection signal was superimposed, and

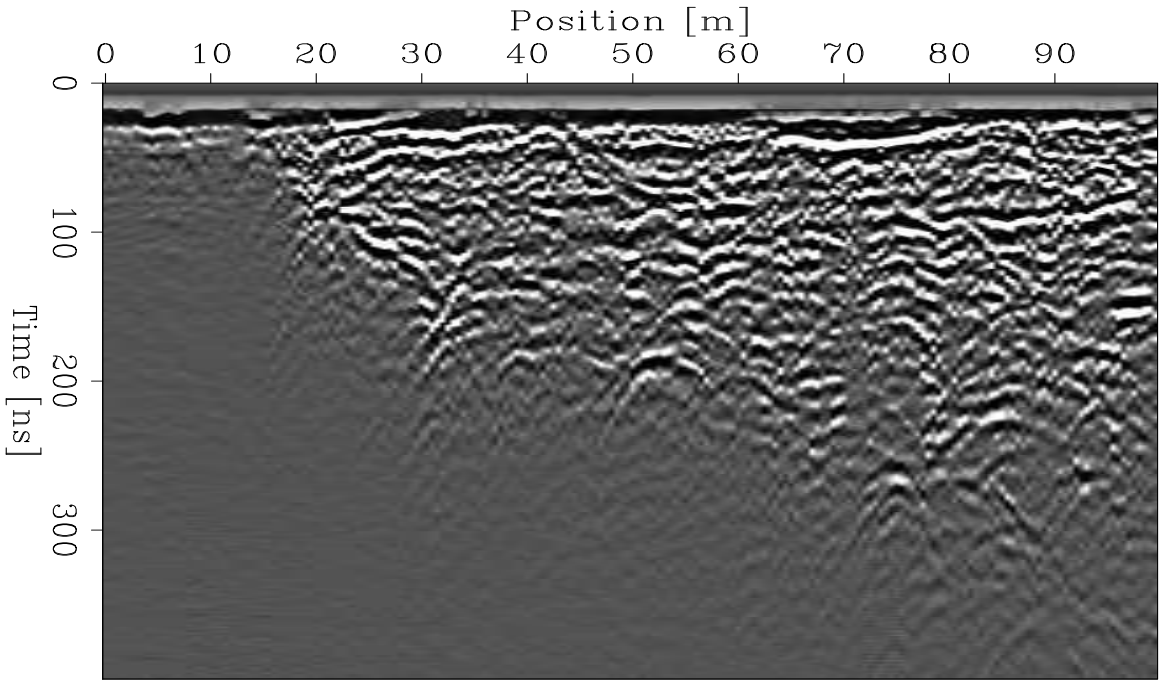

Figure 1: Nearest-offset time section from the Langley multi-offset data set. jeff3-time [ER]

correction for drift in the zero time of the GPR instrument, most likely due to temperature fluctuations. Because the road surface was very flat, no topographic correction was needed. A time-varying exponential gain was also applied to the data to compensate for energy losses incurred by the GPR pulse during propagation.

Figure (1) shows the unmigrated, near-offset (0.5 m) time section extracted from the Langley data set. This is what would be recorded in a typical, constant-offset GPR survey. Notice that the section is quite complicated, with numerous diffraction hyperbolae present and very few laterally continuous reflectors. The dipping boundary between the sand/gravel and clay layers can been seen as the region where the radar signal rapidly attenuates. However, due to the numerous diffraction hyperbolae and conflicting dips present in the section, the exact location of this boundary is difficult to determine.

In order to perform shot-profile migration, a subsurface velocity model was required. To obtain this model, the radar data were sorted into common-midpoint (CMP) gathers, and semblance analysis was performed. After picking the maximum points on the semblance scans, the resulting root-mean-square (RMS) velocity model was interpolated and converted into a map of interval velocity. The resulting model that was used for the migration is approximately $v(z)$, with the boundary between the vadose (high-velocity) and saturated (low-velocity) zones at approximately 4.5 m.

Figure (2) shows the Langley multi-offset data after shot-profile migration. As outlined in the previous section, each shot-gather was migrated through independent extrapolation of the source and receiver wavefields, and application of the imaging condition. The migrated

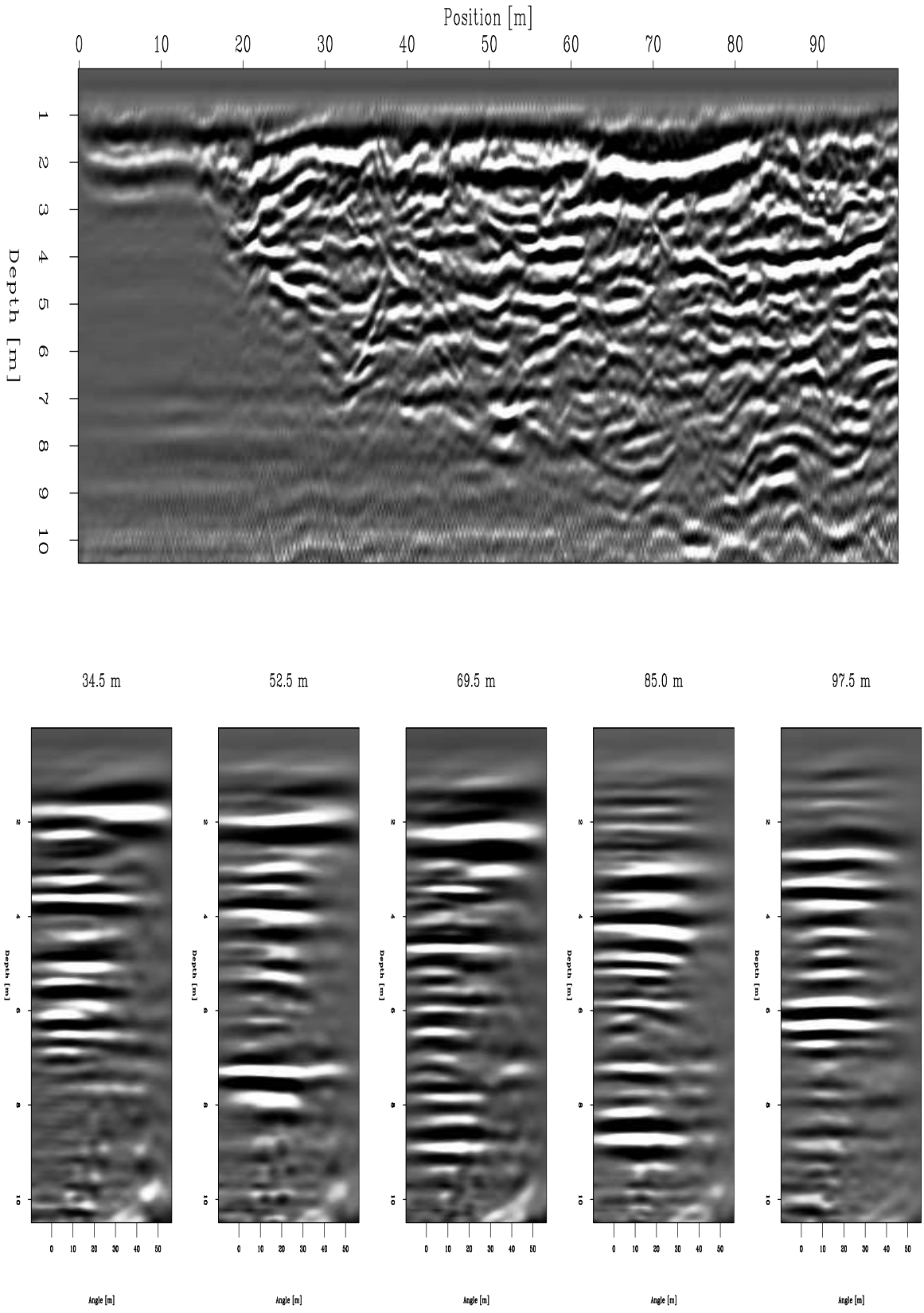

Figure 2: Corresponding depth image after shot-profile migration, and a number of representative ADCIGs. jeff3-depth [CR]

shot gathers were then summed to produce the image shown. Also displayed in Figure (2) are a number of representative ADCIGs from the migrated data. Finite length acquisition leads to a decrease in available incidence angles for reflectors at increasing depth. For this reason, the ADCIGs become less coherent at large angle deeper in the section.

Comparing Figures (1) and (2), notice that the original time section has been significantly improved after shot-profile migration of the multi-offset data. The migrated image is much cleaner, as diffraction hyperbolas have been largely collapsed and conflicting dips due to the interference of diffraction tails have been eliminated. Many laterally continuous reflections which are absent on the time section can now been seen. Most notable is the water table, which is now very visible at approximately 4.5 m depth. Also, the boundary between the sand/gravel and clay layers is easily identified on the migrated section. On-lap of reflectors in the sand and gravel layer with this boundary can also be seen. Finally, notice that the ADCIG panels shown are very flat. This indicates that we have used an appropriate velocity model to image the data. Any remaining curvature in these gathers could be used to further refine this velocity model.

DISCUSSION AND CONCLUSIONS

The seismic community has identified a number of situations where prestack wave-equation migration has advantages over Kirchhoff techniques. The most important of these are the handling of wavefield triplications and earth models with complex structure or large velocity contrasts. Application of the shot-profile migration strategy to GPR shows encouraging results at our field location, and warrants further research. Further, the flexibility of the method allows for incorporation of more accurate source and receiver wavefield modeling, to include effects such as radiation patterns. Lastly, more advanced imaging conditions could be used to incorporate realistic EM scattering physics into the problem.

ACKNOWLEDGMENTS

We would like to thank Dr. Rosemary Knight for the use of the Stanford Environmental Geophysics Research Group's radar system. We also thank Biondo Biondi and Paul Sava for helpful discussions.

REFERENCES

Baker, G., 1998, Applying AVO analysis to GPR data: Geophysical Research Letters, **25**, 397–400.

Claerbout, J., 1971, Toward a unified theory of reflector mapping: Geophysics, **36**, 467–481.

Claerbout, J., 1985, Imaging the earth's interior: Blackwell Science, Inc., New York.

Fisher, E., McMechan, G., and Annan, A., 1992a, Acquisition and processing of wide-aperture ground-penetrating radar data: Geophysics, **57**, 495–504.

Fisher, E., McMechan, G., Annan, A., and Cosway, S., 1992b, Examples of reverse-time migration of single-channel ground-penetrating radar profiles: Geophysics, **57**, 577–586.

Greaves, R., Lesmes, D., Lee, J., and Toksoz, M., 1996, Velocity variations and water content estimated from multi-offset, ground-penetrating radar: Geophysics, **61**, 683–695.

Jackson, J. D., 1975, Classical electrodynamics: John Wiley & Sons, New York.

Rickett, J., and Sava, P., 2002, Offset and angle-domain common image-point gathers for shot profile migration: Geophysics, **67**, 883–889.

Sava, P., and Fomel, S., 2003, Angle-domain common-image gathers by wavefield continuation methods: Geophysics, **68**, 1065–1074.

Sena, A., L., S. P., and K., S. M., 2003, Split step fourier migration of ground penetrating radar data: 73rd Ann. Internal. Mtg. Soc. Expl. Geophys., Expanded Abstracts, pages 1023–1026.

Stoffa, P. L., Fokkema, J. T., de Luna Freire, R. M., and Kessinger, W. P., 1990, Split-step Fourier migration: Geophysics, **55**, no. 04, 410–421.

van der Kruk, J., Wapenaar, C., Fokkema, J. T., and van der Berg, P., 2003, Three-dimensional imaging of multicomponent ground-penetrating radar data: Geophysics, **68**, 1241–1254.